Interfacial reaction phenomenon between La$_{0.25}$Sr$_{0.75}$TiO$_3$ and ScSZ

Gang Chen*, Haruo Kishimoto, Katsuhiko Yamaji, Koji Kuramoto, Teruhisa Horita

National Institute of Advanced Industrial Science and Technology (AIST), AIST Tsukuba Central No. 5, Higashi 1-1-1, Tsukuba 305-8565, Japan

HIGHLIGHTS

- Interfacial reaction between LST anode and ScSZ in air was confirmed.
- La$_2$Zr$_2$O$_7$ (LZO) was identified to be formed at the interface of LST/ScSZ.
- LZO was effectively suppressed when the sample was annealed in H$_2$ atmosphere.
- The interfacial reaction reduced the performance of the cell with LST anode.

ARTICLE INFO

ABSTRACT

Interfacial reaction phenomenon between stoichiometric La$_{0.25}$Sr$_{0.75}$TiO$_3$ (LST) anode and 1CeO$_2$−10Sc$_2$O$_3$−89ZrO$_2$ (ScSZ) electrolyte after annealed at 1200 °C for 30 h in air is investigated. La$_2$Zr$_2$O$_7$ (LZO) phase is found to be formed at the interface of LST/ScSZ via analysis by XRD and SEM measurements. The LZO formation is effectively suppressed when the stoichiometric LST is annealed in reduction atmospheres. The amount of LZO formed at the interface is increased with the annealing time. Based on the experimental results, possible interfacial reaction mechanism between stoichiometric LST and ScSZ electrolyte is proposed.

1. Introduction

One of the important functions of SOFC anode is to supply reaction site for the electrochemical oxidation of fuels. An ideal anode material should have long-term chemical, morphological, and dimensional stabilities in the fuel atmosphere. Compared with the conventional Ni-based composite anode, ceramic anode materials, especially La-substituted-SrTiO$_3$ (LST) perovskite material was found to be tolerable against the sintering of microstructures even after a long-term performance test and provided excellent redox stability over a wide range of oxygen partial pressures (pO$_2$) [1]. As a promising anode material, LST exhibited high electrical conductivity after reduced and similar thermal expansion characterization with doped-zirconia electrolytes (YSZ and ScSZ) [2,3]. Several authors reported that LST had excellent sulphur resistance [4,5], which indicate that LST could be directly fuelled by coal syngas. To

date, the electrochemical performances of LST anodes have been generally performed on electrolyte-supported single cells, and some remarkable power densities have been reported [6,7]. However, the performance of LST composite anodes is still lower than that of Ni-based cermet anodes [8]. The interfacial stability between LST and zirconia electrolyte was considered as one of main suppression mechanisms for the performance of the cell.

It has been known that in ABO$_3$ perovskite oxide family, several materials (LSM, LSC, LSCF, etc.) containing La and Sr elements can react with zirconia electrolytes to form zirconate phases (LZO and SrZrO$_3$) after calcinated at high temperatures [9–12]. In our group, the solid state reaction characterization between YSZ electrolyte and LSM has been experimentally and theoretically studied [13–15]. The thermodynamic calculations indicated that the possibility of formation of LZO at the LSM/YSZ interface is high when (La + Sr) content at the A-site is larger than Mn^{3+} ions at B-site and when Sr/La ratio is smaller than 0.43. And high Sr content will leads to Sr depletion from the lattice and eventual formation of SrZrO$_3$. Lee et al. reported that LZO is so easily formed at the interface of LSM and YSZ even the sample is sintered at a temperature as low as 1000 °C [16].

However, the interfacial stability between stoichiometric LST and doped-zirconia electrolytes is still unclear, although some indirect evidences have already proved that there were no additional phases formed in the physical mixtures of LST and YSZ after annealed at high temperatures [17–19]. Ahn et al. indicated that there was no zirconate phase formed in physical mixture of $La_{0.3}Sr_{0.7}TiO_3$ and YSZ after annealed at 1550 °C for 4 h in air [17]. Sun et al. also found no additional phase peaks in the XRD patterns of $La_{0.4}Sr_{0.6}TiO_3$ and YSZ composite after annealed at 1400 °C for 3 h in air [18]. However, solid state reaction condition between LST powder and ScSZ powder was a little different with that between LST anode film and ScSZ electrolyte substrate. Since the amount of additional phase formed between powder and powder may be only a few while XRD device always has a detection limit, it is difficult to confirm whether the solid state reaction really occurs at the interface of LST anode and ScSZ electrolyte or not. Our previous study found that the secondary phase was formed at interface of stoichiometric $La_{0.25}Sr_{0.75}TiO_3$ anode and $1CeO_2–10Sc_2O_3–89ZrO_2$ (ScSZ) electrolyte after annealed at 1200 °C in air, but there is still no direct data for the phase and composition of such secondary phase [20].

In this study, in order to investigate the detail of interfacial reaction mechanism, half-cell with ScSZ electrolyte and LST anode was annealed at 1200 °C in different atmospheres ($p(O_2) = 0.21$ atm, or $p(O_2) = 2.8*10^{-12}$ atm). XRD and FE-SEM-EDS techniques were used to detect the additional phase formed at the interface of LST/ScSZ. The effect of interfacial reaction on the electrochemical performance of LST anode was investigated through testing the electrochemical performances of three cells with different extent of the interfacial reaction.

2. Experimental

A stoichiometric perovskite of $La_{0.25}Sr_{0.75}TiO_3$ (LST) powder was synthesized by solid state reaction (SSR) method with La_2O_3, TiO_2 and $SrCO_3$ [19]. The starting materials were high purity La_2O_3 (Wako pure chemical industries, Ltd. 99.99%), TiO_2 (Wako pure chemical industries, Ltd. 99.9%), $SrCO_3$ (Rare metallic CO., Ltd. 99.9%). The La_2O_3 powder was pre-calcined at 1000 °C to remove the absorbed moisture. The raw powders were ball milled in ethanol using zirconia balls for 30 min. The powders after ball milled were pressed into pellet and sintered at 1250 °C for 4 h. The pellet was then ground, ball milled, pressed into pellet and sintered at 1250 °C for 4 h again. Such ball milling–grinding–pressing–sintering cycles were repeated for 4 times until no secondary phase was detected. The crystal structure of as-prepared LST was characterized by XRD (Rigaku RINT-Ultima III) with Cu Kα radiation. 0.5 mm thickness of ScSZ, which was prepared by cold isostatic pressing process, was used as electrolyte. As-prepared LST powder was mixed with organic addition agent and prepared into slurry. LST anode slurry was then prepared on ScSZ electrolyte by screen-printing method. To investigate the interfacial reactions, LST anode and ScSZ electrolyte assemblies were annealed in air, in humidified H_2 (1% H_2 + 1.2% H_2O + 97.8% Ar) and in dry diluted H_2 (1% H_2 + 99% Ar) at 1200 °C for 30 h, respectively. The partial pressure of O_2 (pO_2) in humidified H_2 was 2.8×10^{-12} atm. To investigate the effect of interfacial reaction on the electrochemical performance of LST anode, single cells with ScSZ electrolyte and LST anode were annealed at 1200 °C for different periods (2, 4 and 8 h) in air. Platinum electrode was used as cathode. As-prepared single cells with LST anode were performed in H_2 + 1.2% H_2O (humidified at 10 °C) with air in cathode at 1000 °C. The impedances were measured between 0.01 Hz and 1 MHz using Modulab electrochemical system (Solartron analytical) under open-circuit conditions. Each cell was firstly reduced in H_2 + 1.2% H_2O at 800 °C for

about 14 h, and then performed at 1000 °C. Before performance test, each cell was maintained under open circuit state for 1 h until open circuit voltage became stable. Impedance of the cell was then measured, after which I–V curve of the cell was scanned with speed of 1 mV s^{-1} from OCV to 0.6 V and then returned to OCV. The microstructures of the specimens after annealed in different atmospheres and the cells after electrochemical performance test were analyzed by FE-SEM-EDS system.

3. Results and discussion

3.1. Interaction between LST and ScSZ powders

Fig. 1 shows XRD patterns of as-prepared LST powder and LST/ScSZ composite pellet after annealed at 1200 °C for 30 h in air. Measurements were carried out for 2θ values between 20 and 90° by conventional θ–2θ geometry method. As indicated in Fig. 1(a), the peaks splitting (induced by two kinds of X-ray, Kα1 and Kα2) were observed at high angel range (60–90°), which confirmed that cubic perovskite structure was formed in as-prepared LST after several ball milling and sintering cycles. In order to investigate the chemical reaction phenomenon between LST and ScSZ powders, LST/ScSZ composite powders (physical mixture) with weight ratio of 1:1 were pressed into pellet and sintered at 1200 °C for 30 h in air. The XRD pattern of the surface of pellet after annealed was shown in Fig. 1(b). No zirconate phase (LZO or $SrZrO_3$) was found, which was consistent with the results reported in some Refs. [17–19]. The broadening peak of LST in LST/ScSZ composite pellet (as indicated in Fig. 1(b)) indicated that the interaction between LST and ScSZ was existed after annealed at 1200 °C in air. Since XRD device has the detection limit, it is difficult to direct confirm if the solid state reaction really occurs at the interface of LST anode and ScSZ electrolyte. Therefore the direct evidence from interface of LST/ScSZ is needed.

3.2. Interfacial reaction between LST anode and ScSZ electrolyte

Fig. 2 shows SEM cross section images (with backscattered electron) of the pellets with LST anode and ScSZ substrate after annealed in air (a), in 1% H_2 + 1.2% H_2O + 97.8 % Ar (b) and in dry 1% H_2 + 99% Ar (c) at 1200 °C for 30 h, respectively. From Fig. 2(a), white phase was observed at the interface of LST/ScSZ. A dense grey phase layer was formed on the layer of LZO at interface of LST/ScSZ.
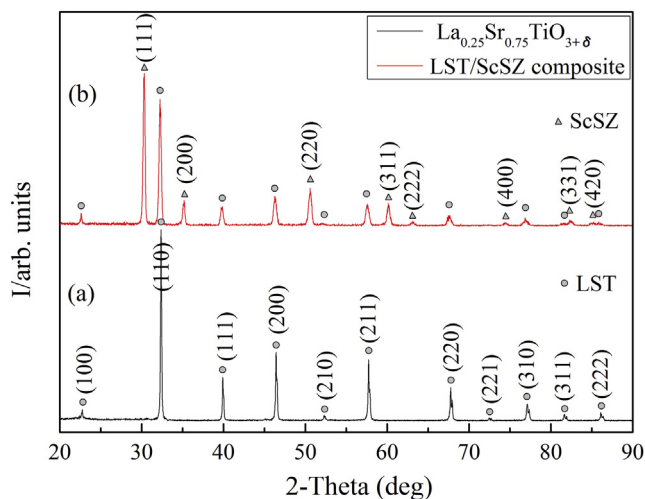

Fig. 1. XRD patterns of as-prepared LST powder (a); and the LST/ScSZ composite pellet after annealed at 1200 °C for 30 h in air (b).
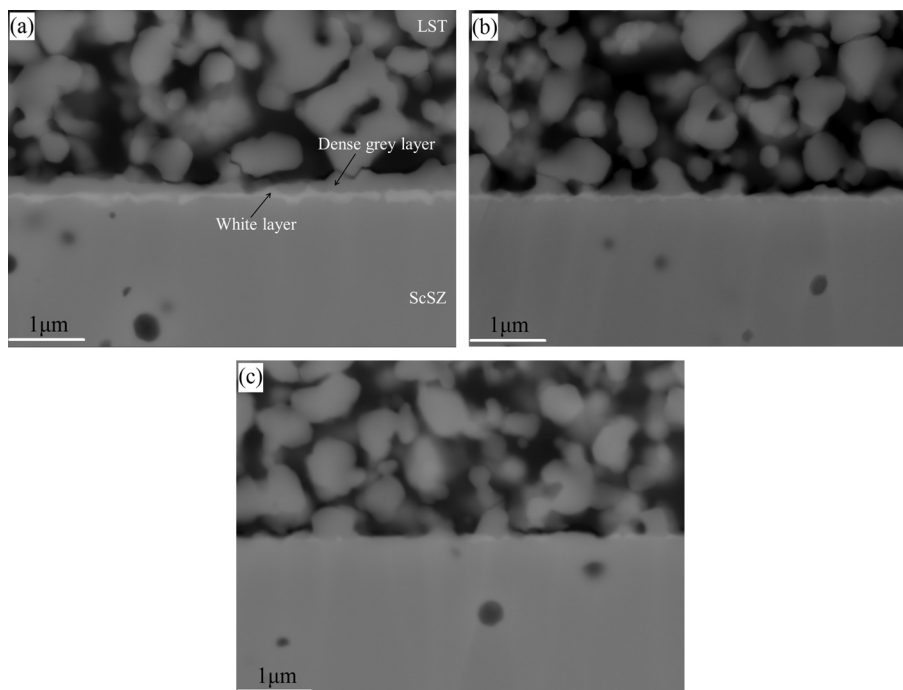
Fig. 2. SEM images of cross section of the pellets with LST anode after annealed at 1200 °C for 30 h in different atmospheres, (a) in air; (b) in humidified H_2 ($pO_2 = 2.8*10^{-12}$ atm) and (c) in dry 1% H_2 + 99% Ar.

The formation of white phase and dense grey phase indicate that the interfacial reaction should be occurred between LST and ScSZ after annealed at 1200 °C in air. The amount of white phase in Fig. 2(b) was obviously less than that in Fig. 2(a). Only a few amount of white phase was observed in Fig. 2(c), indicates that the reduction of partial pressure of oxygen in annealing atmosphere can effectively suppress the interfacial reaction between LST and ScSZ when the pellet was annealed at 1200 °C.

Fig. 3 shows the elemental maps of the half-cell pellet with LST anode after annealed at 1200 °C for 30 h in air. The highlighted La was found at the white phase, which indicated that La was one of the main constitutions of the white phase. Thus, LZO was considered to be the main composition of the white phase. The results of element point analysis (cation at.%) correspond to the SEM image of Fig. 3 were shown in Table 1. As indicated in the SEM image of Fig. 3, the thickness of white phase layer was about 100 nm, thus the cation atomic percentage shown in spectrum 5 and spectrum 6 should partly from ScSZ electrolyte and dense grey phase due to the detection limit of EDX point analysis. The inter-diffusion of La, Sr and Ti into ScSZ and Zr, Sc into LST where close to the interface of LST/ScSZ should be happened due to the interfacial reaction after sintered at 1200 °C. The constitution of dense grey phase should be La–Sr–Ti–Zr–Sc–O solid solution and/or Zr and Sc doped LST.

In the present case, the white phase formed between LST and ScSZ was ultra thin, which was not easy to be detected by conventional $\theta-2\theta$ geometry XRD method. Thus, a grazing incidence diffraction method of XRD with 3° grazing incidence was used to characterize the white phase. Measurements were carried out for 2θ values between 20 and 60°. Fig. 4 shows the XRD pattern (grazing incidence method) of the inside surface of ScSZ substrate (annealed in air) after the LST anode was removed. LZO was confirmed to be formed at the surface of ScSZ. No $SrZrO_3$ was observed. Little TiO_2 phase was found in XRD pattern. Two conjoint peaks were observed at 46 and 57.5°, respectively, which were considered as the peaks of $SrTiO_3$ and LST, respectively. From this result, we confirmed that interfacial reaction between LST and ScSZ was existed.

Until now there is still no theoretical explanation on the solid state reaction mechanism between LST and zirconia electrolyte. The already known knowledge on the interfacial reaction between LXM (X = Sr, Ca or none element) and YSZ could be used as reference for the explanation of the interaction of LST and ScSZ [21]. Roosmalen and Cordfunke investigated the chemical reactivity and inter-diffusion of (La, Sr)MnO$_3$ and (Zr, Y)O$_2$ from 1110 to 1755 K, and found that the formation of LZO and/or $SrZrO_3$ between LaMnO$_3$ with (Zr, Y)O$_2$ was happened at 1170 K [10]. They proposed that solid reactions were formed by diffusion of La and/or Sr into (Zr, Y)O$_2$ via a vacancy diffusion mechanism. Taimatsu et al. studied the reaction of $La_{1-x}Ca_xMnO_3$ (x = 0, 0.1, 0.2) with YSZ in the temperature range of 1300–1425 °C in air [9]. They found that the reaction proceed by unidirectional diffusion of La, Mn, and/or Ca ions, mainly Mn ions, into YSZ. The amount of Mn ion diffused into YSZ was far more than that of the La ion diffused into YSZ, which resulted in the excess of La at the reaction interface, and eventually leading to the formation of LZO layer at the interface. Mitterdorfer and Gauckler also reported that the excess lanthanum oxide within the perovskite reacted immediately with YSZ to form dense LZO [12]. They prepared the porous $La_{0.85}Sr_{0.15}Mn_yO_{3+\delta}$ (y = 0.95…1.1) perovskites on YSZ and sintered in air at 1373 K for short periods, and found that the growth of LZO is controlled by bulk diffusion of cations.

In the present case, the formation of LZO at interface of LST/ScSZ indicates that the chemical reactivity of La in stoichiometric is high enough to react with Zr in ScSZ after annealed at 1200 °C under high oxygen partial pressure atmosphere. According to the XRD result showed in Fig. 4 and the elemental maps results indicated in Fig. 3, possible reaction occurred at interface of LST/ScSZ after annealed at high temperature in air was expressed as following:

$$La_{0.25}Sr_{0.75}TiO_3 + 1/4ZrO_2 + 1/16O_2 \rightarrow 1/8LZO + 3/4SrTiO_3 + 1/4TiO_2 \tag{1}$$
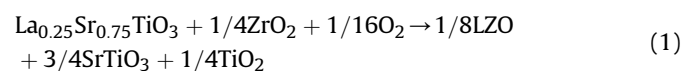
The annealing atmosphere and temperature are two main factors for the formation of LZO at the interface of LST and ScSZ.
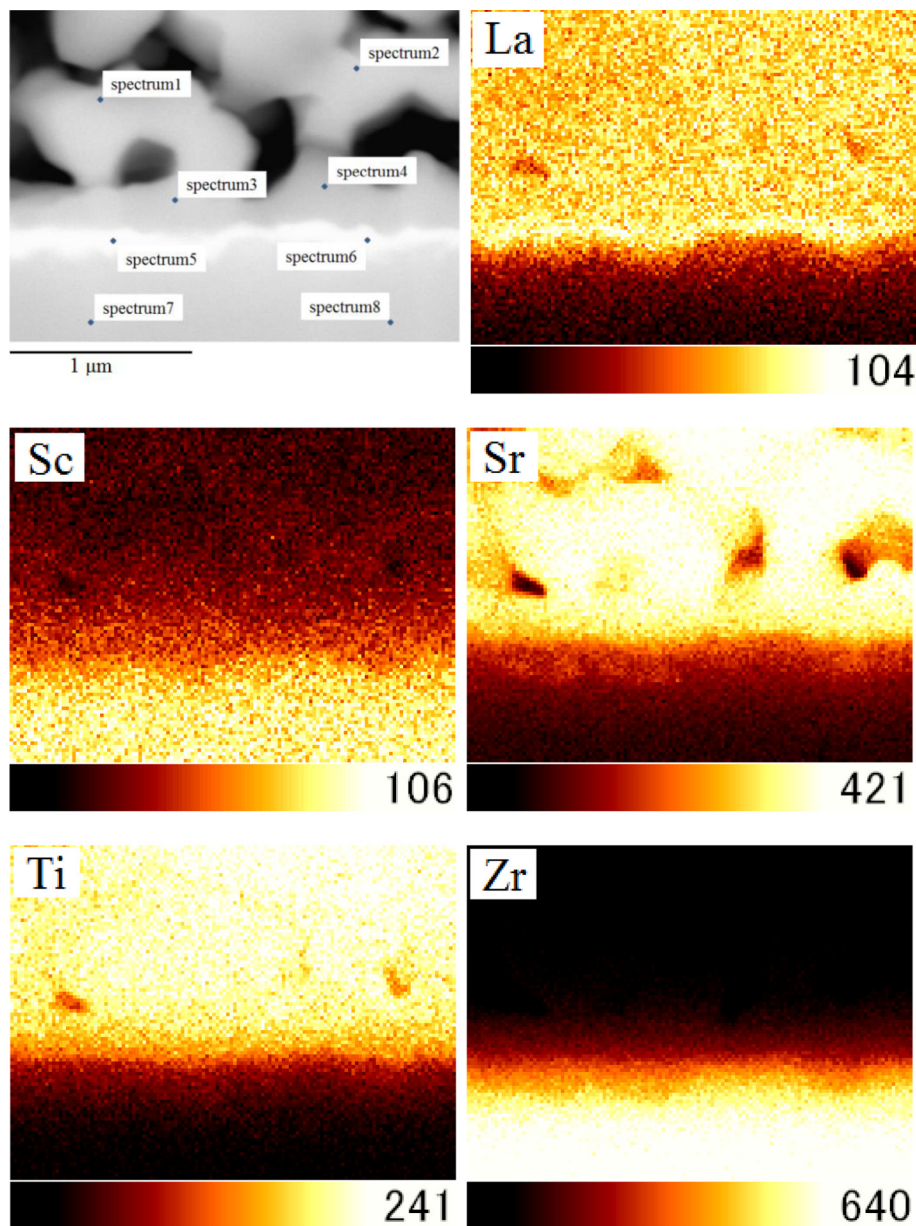
Fig. 3. Elemental maps of the high magnification of cross section of the pellet with LST anode after annealed at 1200 °C for 30 h in air.

From reaction Equation (1) we can understand why the low oxygen partial pressure atmosphere could suppress the interfacial reaction between LST anode and ScSZ electrolyte. On the other hand, the inter-diffusion of elements nearby interface which was induced by

Table 1
Results of point elemental analysis (cation at.%) of the pellet with ScSZ electrolyte and LST anode after annealed at 1200 °C for 30 h in air.

Spectrum no.	Elemental (cation at.%)					
	La	Sr	Ti	Sc	Zr	Ce
Spectrum 1	8.3	38.6	45.4	1.7	6.1	0
Spectrum 2	9.5	39.0	47.3	0.6	3.5	0
Spectrum 3	9.7	29.4	33.7	4.7	22.4	0
Spectrum 4	9.8	32.6	38.0	3.1	16.5	0
Spectrum 5	13.8	14.2	11.7	7.4	52.1	0.8
Spectrum 6	12.8	14.0	11.8	8.6	52.5	0.3
Spectrum 7	0.9	2.6	1.0	15.4	79.8	0.4
Spectrum 8	1.1	3.3	1.8	14.7	78.4	0.6

the interfacial reaction also has effect on the formation of LZO. The diffusion of Ti, Sr and La into ScSZ could change the stoichiometric number of La in LST, and eventually change the reactivity of La in LST. Several authors reported that Ti was easily diffused from doped-SrTiO$_3$ into zirconia electrolyte after sintered at high temperatures, which could increase the reactivity of La in LST [2,22]. Burnat et al. investigated the chemical reactivity between A-site deficient La$_{0.2}$Sr$_{0.7}$TiO$_3$ (LST$_{27}$) and zirconia electrolyte materials (YSZ and ScSZ) in oxidation and reduction atmospheres at much higher temperature (1400 °C), respectively [22]. Their results indicated that no LZO was formed at interface of A-site deficient LST and zirconia electrolyte material after annealed at 1400 °C. Our previous study also found that A-site deficient LST could effectively suppress the interfacial reaction between LST anode zirconia electrolyte, and the chemical reactivity of La in La-substituted-SrTiO$_3$ is reduced with increasing A-site deficiency [20].

To investigate the effect of the interfacial reaction during cell preparation on the electrochemical performance of LST anode,
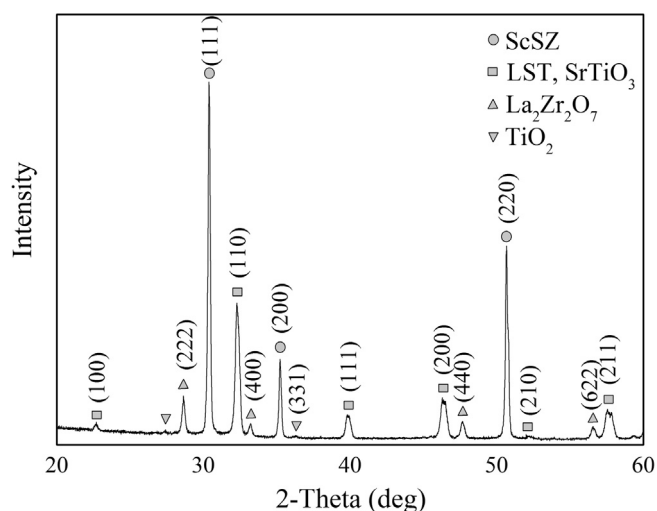
Fig. 4. XRD pattern of the surface of ScSZ after the LST anode was removed (the assembly annealed for 30 h in air).

three cells with different extent of interfacial reaction (controlled by anode sintering time) were performed in humidified H_2. Fig. 5(a) and (b) shows the typical *IV* curve and impedance spectra of the cells with LST anode sintered at 1200 °C in air for different periods (2, 4 and 8 h) and operated at 1000 °C, respectively. In this study, to avoid the effect of performance degradation of LST anode occurred during long-term performance test, all cells were performed in a short period after anode reduction process. Electrochemical performance difference of the cells was considered to be induced by the differences of the cells induced during cell preparation process (anode annealing process). From Fig. 5(a), one can see that the current density of the cell with LST anode at same voltage decreased with the increasing of anode annealing time (1200 °C in air). As indicated in Fig. 5(b), the ohmic resistance (R_o) of the cells with 2, 4 and 8 h anode annealing time were 0.268, 0.239 and 0.216 Ω cm^2, respectively. Fig. 6 shows backscattered electron cross section SEM images of the cells with LST anode sintered at 1200 °C for different periods (2, 4 and 8 h). From the figures, white phase was observed at the interface of LST/ScSZ in each sample. The amount of LZO phase increased as annealing time increased. However, the increasing of LZO phase as anode annealing time did not leading to the increasing of R_o. In the present case, the thickness of ScSZ electrolyte was 0.5 mm. The conductivity of ScSZ was about 0.3 S cm^{-1} at 1000 °C [23]. The ohmic resistance of ScSZ electrolyte was about 0.167 Ω cm^2, which was calculated according to the effective area of anode and the thickness of ScSZ. Thus, the main part of R_o was from ScSZ electrolyte in the present case, although the electrical conductivity of LZO was 2.5×10^{-5} S cm^{-1} which was 4–7 orders of smaller than those of ScSZ electrolyte and LST anode [16]. The thickness of LZO film was very thin, the LZO layer was a mixture layer, and the connectivity of LST and LST in anode and the connectivity between LST anode and ScSZ electrolyte became better with the increasing of annealing time (the area of contact surface between LST and ScSZ increased). These were considered as the main reasons for the reducing of R_o as the increasing of annealing time. In present case, it is difficult to use R_o to explain the current density decreasing phenomenon for the cell with various LST anodes annealing time here. It should be noted that the difference between the high frequency and low frequency intercepts on the real axis represent the polarization resistance (R_p) [24], which was increased with the increasing of anode annealing time. As reported so far, LST has very low ionic conductivity with poor
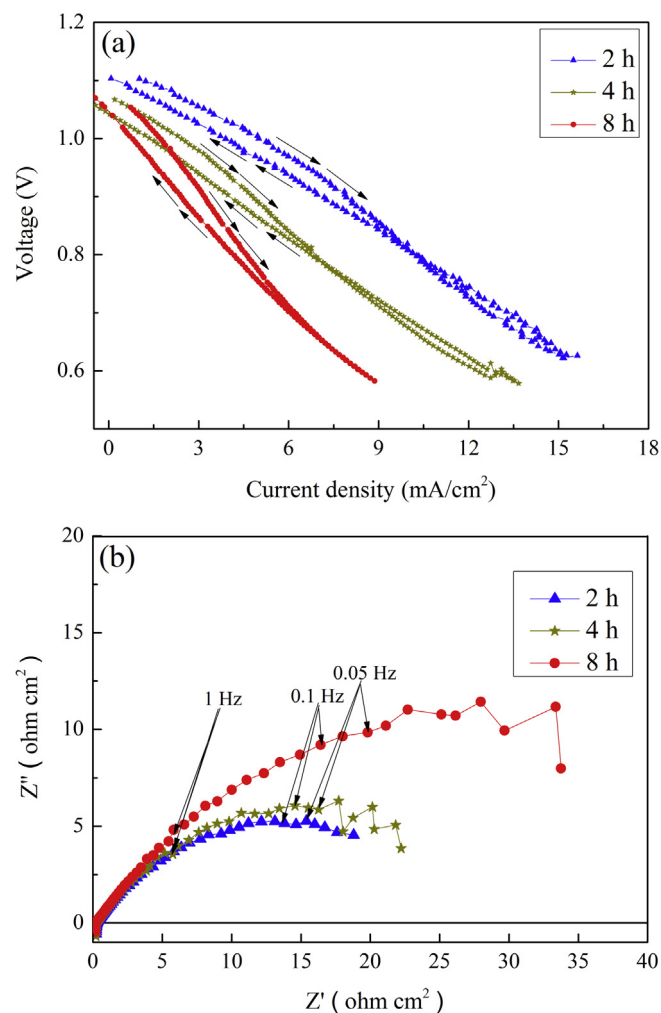

Fig. 5. (a) *IV* curves of the cells with LST anode sintered at 1200 °C for different periods (2, 4 and 8 h) operated at 1000 °C; (b) Impedance spectra of the cells with LST anode sintered at 1200 °C for different periods (2, 4 and 8 h) measured under open circuit state at 1000 °C.

electro-catalytic performance [18]. Therefore, the active reaction zone of LST anode should be limited to the TPB of fuel/LST/ScSZ interfaces.

Fig. 7 shows the diagram of the reaction mechanism of H_2 and O^{2-} in a SOFC with LST anode. The adsorption and catalytic reaction of H_2 and the oxidation reaction of H and O^{2-} were occurred at TPB in sequence. In present case, the electrochemical reactions occurred at TPB could be significantly affected by the formation of LZO with poor electro-catalytic performance and low electrical conductivity. On the other hand, the formation of dense grey phase on the layer of LZO reduced the area of TPB (fuel/LST/ScSZ) (as indicated in Fig. 6(b) and (c)), which may also have great negative effect on the electrochemical reactions occurred at TPB of the cell. The effect of dense grey phase (La–Sr–Ti–Zr–Sc–O solid solution and/or Zr and Sc doped LST) on the electrical performance of LST is still unclear. Further study is needed to clarify if the doping of Sc and Zr into LST can reduce the electronic conductivity or increase the ionic conductivity or not. The poor electro-catalytic performance of LZO and the dense grey phase, as well as the decreasing of the amount of active site to the oxidation of H_2 due to interfacial reactions led to the increasing of R_p and eventually reduce the performance of the cell.
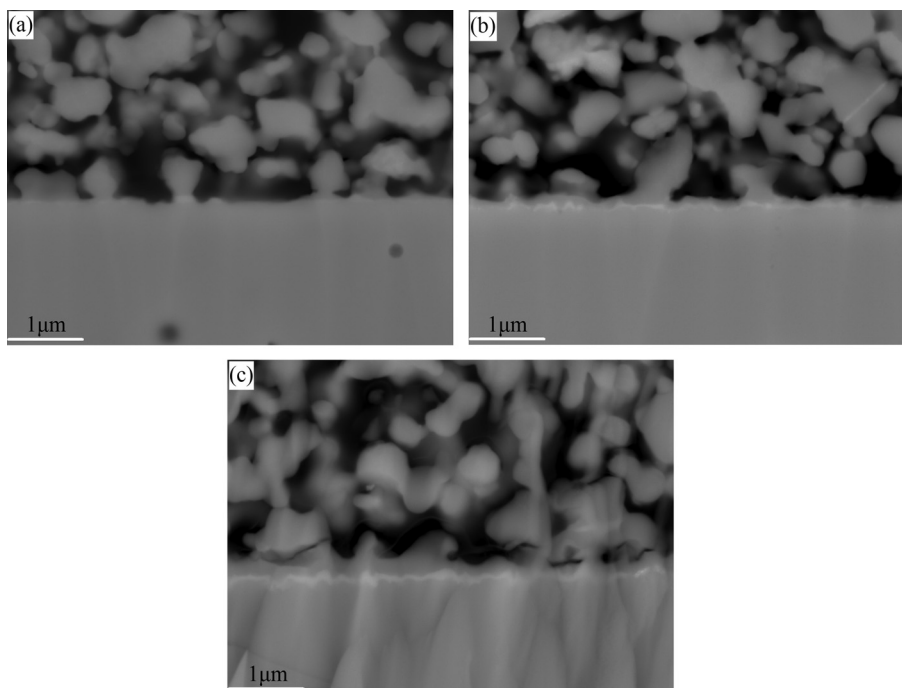
Fig. 6. SEM images of cross section of the cells with LST anode sintered at 1200 °C for different periods, (a) 2 h, (b) 4 h and (c) 8 h.
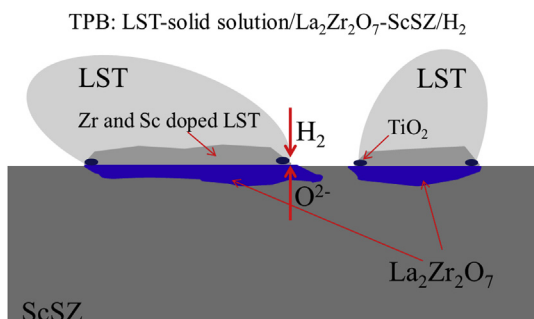

Fig. 7. Diagram of the reaction mechanism of H_2 and O^{2-} in SOFC with LST anode.

4. Conclusions

Stoichiometric LST with cubic perovskite structure was prepared by solid state reaction method. Interfacial reactions between LST and ScSZ were investigated by annealing the assemblies of LST on ScSZ substrate at 1200 °C in different atmospheres. The formation of LZO at the interface of LST/ScSZ was observed in each sample. The reduction atmosphere was found to suppress the interfacial reactions between LST and ScSZ. SEM results indicated that the solid state reaction between LST and ScSZ was affected by the annealing atmosphere and annealing time. The decreasing of TPB area and the formation of LZO due to the interfacial reaction eventually reduced the performance of the cell with LST anode.

Acknowledgements

References

[1] D. Burnat, A. Heel, L. Holzer, D. Kata, J. Lis, T. Graule, J. Power Sources 201 (2012) 26–36.
[2] Q. Ma, F. Tietz, D. Sebold, D. Stöver, J. Power Sources 195 (2010) 1920–1925.
[3] M. Mori, T. Yamamoto, H. Itoh, H. Inaba, H. Tagawa, J. Electrochem. Soc. 145 (1998) 1374–1381.
[4] M. Roushanafshar, J.L. Luo, A.L. Vincent, K.T. Chuang, A.R. Sanger, Int. J. Hydrogen Energy 37 (2012) 7762–7770.
[5] R. Mukundan, E.L. Brosha, F.H. Garzon, Electrochem. Solid-State Lett. 7 (1) (2004) A5–A7.
[6] C.D. Savaniu, J.T.S. Irvine, Solid State Ionics 192 (2011) 491–493.
[7] J.C. Ruiz-Morales, J. Canales-Vázquez, C. Savaniu, D. Marrero-López, W. Zhou, J.T.S. Irvine, Nature 439 (2006) 568–571.
[8] P. Cowin, C.T.G. Petit, R. Lan, J.T.S. Irvine, S.W. Tao, Adv. Energy Mater. 1 (2011) 314–332.
[9] H. Taimatsu, K. Wada, H. Kaneko, H. Yamamura, J. Am, Ceram. Soc. 75 (1992) 401.
[10] J.A.M. van Roosmalen, E.H.P. Cordfunke, Solid State Ionics 52 (1992) 303.
[11] G. Stochniol, E. Sysakis, A. Naoumidis, J. Am. Ceram. Soc. 78 (1995) 929.
[12] A. Mitterdorfer, L.J. Gauckler, Solid State Ionics 111 (1998) 185–218.
[13] H. Yokokawa, N. Sakai, T. Kawada, M. Dokia, J. Electrochem. Soc. 138 (1991) 2719–2727.
[14] H. Yokokawa, T. Horita, N. Saka, M. Dokiy, T. Kawada, Solid State Ionics 86–88 (1996) 1161–1165.
[15] T. Kawada, N. Sakai, H. Yokokawa, M. Dokia, Solid State Ionics 52 (1992) 189–196.
[16] H.Y. Lee, S.M. Oh, Solid State Ionics 90 (1996) 133–140.
[17] K. Ahn, S. Jung, J.M. Vohs, R.J. Gorte, Ceram. Interface 33 (2007) 1065–1070.
[18] X. Sun, S.R. Wang, Z.R. Wang, X.F. Ye, T.L. Wen, F.Q. Huang, J. Power Sources 183 (2008) 114–117.
[19] C.D. Savaniu, J.T.S. Irvine, J. Mater. Chem. 19 (2009) 8119–8128.
[20] G. Chen, H. Kishimoto, K. Yamaji, K. Kuramoto, T. Horita, ECS Trans. 50 (2013) 63–71.
[21] S.P. Jiang, J. Mater. Sci. 43 (2008) 6799–6833.
[22] D. Burnat, A. Heel, L. Holzer, E. Otal, D. Kata, T. Graule, Int. J. Hydrogen Energy 37 (2012) 18326–18341.
[23] O. Yamamoto, Y. Arati, Y. Takeda, N. Imanishi, Y. Mizutani, M. Kawai, Y. Nakamura, Solid State Ionics 79 (1995) 137–142.
[24] Y.H. Heo, J.W. Lee, S.B. Lee, T.H. Lim, et al., Int. J. Hydrogen Energy 36 (2011) 797–804.